ATOMISTIC MODELING OF CONDUCTION AND DIFFUSION IN POLYMER ELECTROLYE FUEL CELLS

Xiangyang Zhou
Department of Mechanical and Aerospace Engineering
University of Miami
P.O.Box 248294, Coral Gables, Fl 33157
Tel/Fax: (305) 284-3287/(305) 284-2580; E-mail: xzhou@miami.edu

Abstract

The present paper reports recent results and new findings in molecular dynamic (MD) modeling of the polymer electrolyte and catalyst layer with nanoscale structures in polymer electrolyte fuel cells (PEFCs), namely: 1) proton conduction and diffusion in free Nafion electrolyte clusters; 2) diffusion in the nanoscale interfacial area between a Nafion cluster and carbon support; and 3) disintegration and re-precipitation of Pt nanocrystallities interfacing with Nafion electrolyte. The simulations can predict the conductivity and/or diffusivity of hydronium, water, and methanol in the nanoscale water containing networks of Nafion in a temperature range between 20 and 120 °C. The simulations show that vibrations of the nanoscale carbon support strongly impact diffusion in the Nafion electrolyte interfacing with the carbon support and enhance the diffusivity of hydrogen, oxygen, methanol, water, and hydronium by up to 8 times. However, charging the carbon support reduces the diffusivities. It was found that charging of nanoscale Pt catalysts under a realistic potential drop (0.5 V) resulted in disintegration of the Pt catalysts leading to a reduction of catalytic activity of the catalyst layer. Pre-precipitation of the Pt atoms under a discharging condition can also be simulated using the MD modeling method.

KEYWORDS

Molecular dynamic modeling, transport processes, nanoscale structure, polymer electrolyte, catalyst layer.

INTRODUCTION

Polymer electrolyte fuel cell (PEFC) is considered as the most promising power source for futurist's hydrogen economy. As shown in Fig. 1, operation of a PEFC is dictated by electrochemical reactions at catalyst/polymer electrolyte interfaces and transport processes in the polymer electrolyte membrane (PEM), in the catalyst layers consisting of precious metal (Pt or Ru) catalysts on porous carbon support and polymer electrolyte clusters, and in gas diffusion layers (GDLs).

Nafion, a sulfonated tetrafluorethylene copolymer and the most commonly used polymer electrolyte, consists of nanoscale hydrophobic domains and proton conducting hydrophilic domains. The diffusivities of the reactants (O_2, H_2, and methanol) and products (water and CO_2) in Nafion and proton conductivity of Nafion strongly depend on the hydration level, λ. Ideal power density and catalyst utilization can be achieved on a delicate balance between water production, water transport, reactant diffusion, and proton conduction in catalyst layer containing nanoscale Nafion clusters, carbon supports, and Pt catalysts.

Nafion clusters in the catalyst layers also play a critical role in the degradation of the Pt catalysts. Polymer electrolyte participates in the initial dissolution and/or disintegration of the Pt catalysts during charging and discharging cycles. Transport of the Pt ions and precipitation of these Pt ions in the polymer electrolyte is one of the controlling factors for the loss of electrochemical activity (ECA) of the Pt catalysts.

There are two categories of simulation models for the transport processes in PEFCs: continuum physical models [1, 2] and atomistic models [3-8]. The continuum physical models use the continuous functions and differential equations to describe the transport properties and transport processes in GDLs, in catalysts layers, and in Nafion electrolyte. These models are created with a series of assumptions, hypotheses, empirical laws, and pre-determined properties and parameters that may or may not have well defined physical meaning. The effective properties of the materials are average values over a macroscopic space that encompasses both large (micrometers) or small (nanometers) domains or phases. In Nafion, there are proton-conducting hydrophilic domains and non-conducting

hydrophobic domains with size of a few nanometers. In the catalysts layer, there are carbon particles (support) with pores of a few nanometers. Nafion clusters fill the nanoscale pores and gaps between the carbon particles and form the paths for transport processes. Only the Pt nano-crystallities on the carbon support and in contact with the Nafion clusters can enable electrocatalysis for power generation. Although continuum models may serve well as tools for describing the transport processes in flow channels and in GDLs in which the characteristic size is 10 micrometers, they are inadequate for describing the transport processes in nanoscale structures.

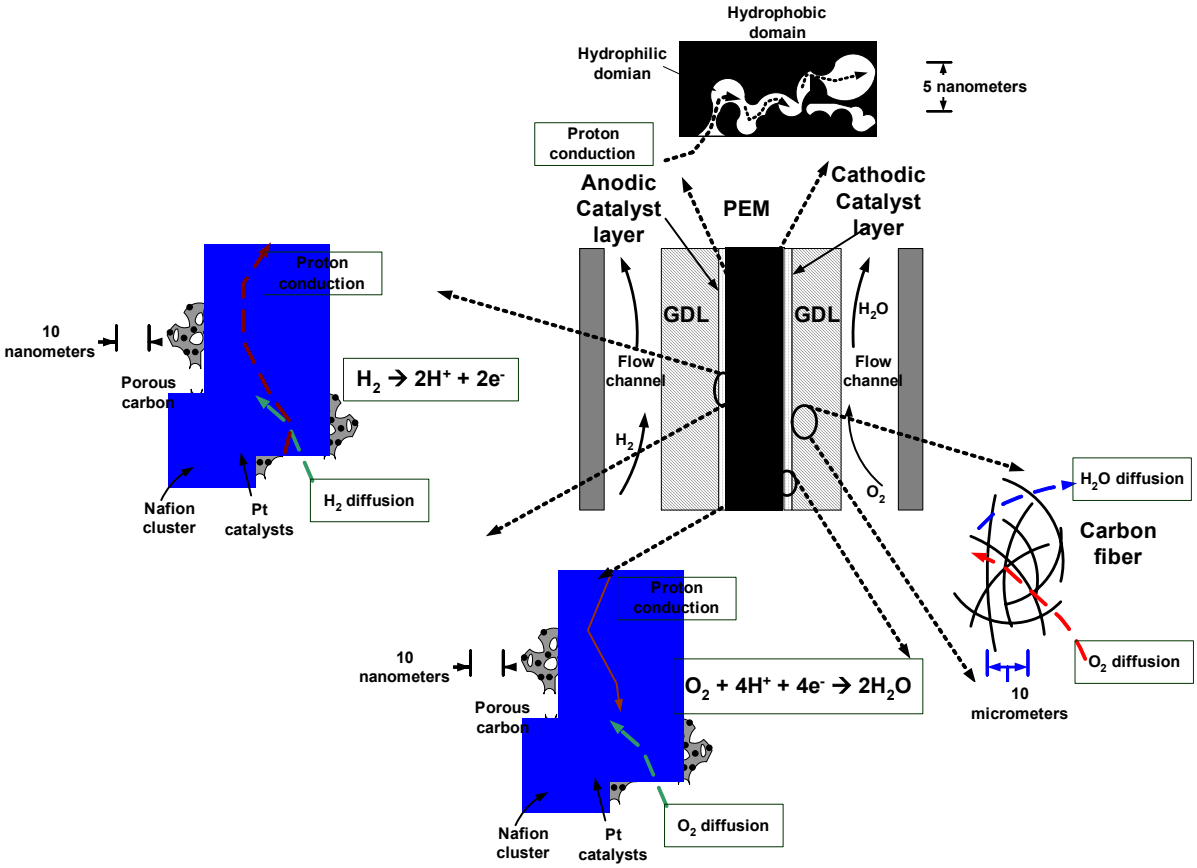

Fig. 1. Schematic illustration of electrochemical and transport processes in a PEFC

Atomistic simulation methods include both classical and *ab initio* quantum mechanics methods. The *ab initio* methods based on Schrödinger equation are "exact" in the sense that they can be as accurate as possible, only subject to computational time or computational resource limitations. In this regard, *ab initio* molecular dynamics (AIMD) methods can evaluate the forces acting the nuclei from the electronic structure calculations that are performed as the trajectory of the molecules is generated [3, 7, 8]. Due to the high demand for the computational resources, AIMD methods are limited to analyses of small clusters (a few nanometers) and within a very short period of time (a few picoseconds) that are unable to represent real-world materials and phenomena. These methods are now being used for elucidating the mechanisms of physicochemical processes or for providing qualitative predictions.

Classical dynamic simulation methods or classical molecular dynamic (MD) methods are based on the Newton's second law and inter-atom force fields that are evaluated using quantum mechanics [9]. Thus, these methods usually do not allow analysis of the chemical reactions that involve chemical bond breaking or formation, as those in the structural diffusion of protons via Grotthuss mechanism [3, 4]. However, in comparison to the *ab initio* methods, the MD methods require much less computational resources and are able to analyze a models with a realistic size but still can achieve a sufficient precision in analyzing, in particular, the "vehicular diffusion" that dominates at lower hydration levels. These methods are particularly suitable for analyzing phenomena in the systems with a size up to 100 nanometers and characteristic time up to a few nanoseconds. The sizes of Nafion

clusters and carbon supported catalysts are in this range. MD modeling of the catalyst layer may directly establish the relationship between microscopic properties and macroscopic properties that can be used by the continuum models to carry out a hierarchical multiscale modeling.

The present paper reports recent results and findings in MD modeling of 1) proton conduction and mass transport in free Nafion electrolyte clusters; 2) diffusion at the interfacial area between a Nafion cluster and carbon support; and 3) disintegration and re-precipitation of Pt catalysts interfacing with Nafion electrolyte.

PROTON CONDUCTION AND MASS TRANSPORT IN FREE NAFION ELECTROLYTE CLUSTERS

Molecular Dynamic Models

The molecular models (unit cells) were constructed using Materials Studio™ with quantum chemistry and MD modules. The first step was to construct individual molecules including H_2O, H_3O^+, H^+, methanol, and Nafion repeating units. Hydronium is more stable and mobile than other hydrated water clusters [10]. Thus, protonated water clusters other than hydronium were not considered in the simulations. Although in reality, the bonds in hydronium can undergo formation or cleavage, the bonds remain intact in the present MD simulations because the simulations purport to evaluate the contribution of the "vehicular diffusion" versus the structural diffusion. The second step is to make a Nafion backbone with two branches. In the third step, these molecules were optimized using the quantum chemistry module (VAMP™) to achieve minimum total energies. Then, using the MD simulation module, Discover™, the optimized molecules were included into a molecular model of Nafion or a unit cell for a periodic boundary condition. Finally, the unit cell was then optimized in the pcff force field [11] using NVT ensembles at different temperatures to allow the total interaction potential to converge to a minimum. The duration time was typically 0.2 ns.

The water content in the unit cells in **Fig. 2** is defined as the molar ratio of water to the sulfonated group in Nafion and expressed as an empirical function of relative humidity according to the experimental data presented in Refs. [1] and [2]. At a relative humidity of 50% the water content is ca. 3 and in liquid water the corresponding water content is ca. 22. The density of Nafion, ρ, is a function of water content, λ [1, 2]:

$$\rho = \frac{EW + M_0\lambda}{V_m + \lambda V_0}, \qquad [1]$$

where EW is the equivalent weight of Nafion 117 or 1100 g mol^{-1}, V_m is the partial molar volume of the dry membrane, or,

$$V_m = \frac{EW}{\rho_{m,0}}. \qquad [2]$$

V_0 is the molar volume of water in Nafion, M_0 is the equivalent weight of water, and $\rho_{m,0}$ is the density of dry membrane, or 2.0 g·cm^{-3}. As shown in Fig. 2, in the unit cell with water content of 3 there are water channels separated by hydrophobic Nafion backbones whereas in the unit cell with water content of 22 the hydrophilic domains overwhelm the Nafion backbones. Each sulfonated group (-SO_3) do attract several water or hydroniums in its vicinities.

Three unit cells were used for the MD simulation. Their water uptakes or water contents were 3, 13, or 22 H_2O/SO_3^-, which correspond to the room temperature water uptakes at 50 % relative humidity (RH), at 100 % RH, and in liquid water respectively [1, 2]. The temperature was initially set at a value between 298.15 and 423.15 K under NVE ensemble with constant particle number, constant volume (1 bar), and constant energy. However, the final temperature was usually different from the initial temperature. The initial velocity was randomly determined according to Boltzmann statistics. The time step was set at 1.0 fs and duration was 100 ps.

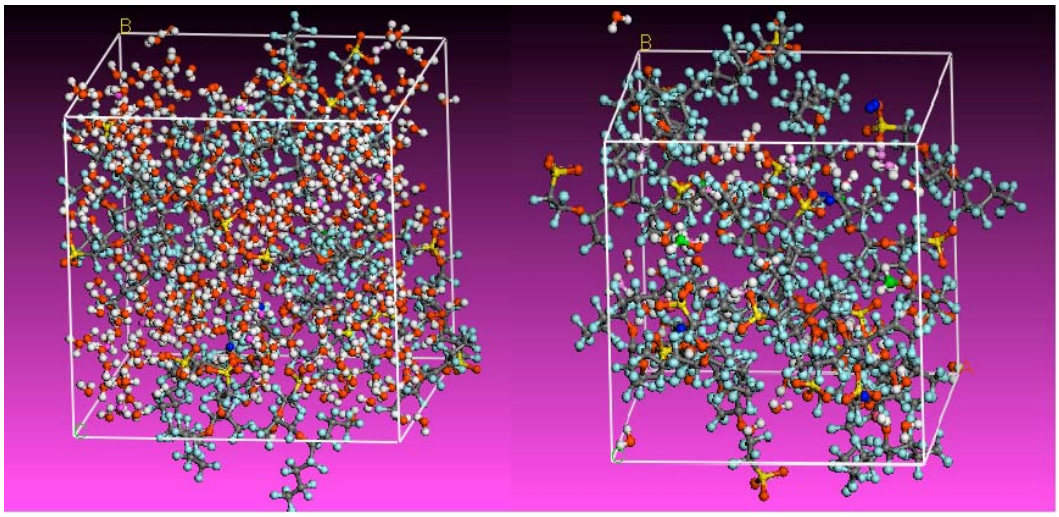

Fig. 2. Two model repeating unit cells. Left: λ = 22; and right: λ = 3

Molecular Dynamic Simulation Results

Each run of the molecular dynamic (MD) computation lasts about 48 hours using a Dell Pentium IV personal computer. The position vector of each particle, $R_i(t)$, is saved as a function of time. The diffusivity of a specific molecule or ion was evaluated using [10, 11]:

$$D_a = \frac{1}{6N_a}\lim_{t\to\infty}\frac{d}{dt}\sum_{i=1}^{N_a}\left\langle [R_i(t) - R_i(t)]^2 \right\rangle, \qquad [3]$$

where N_a is the number of diffusing molecules. The sum term on the right side divided by N_a is the mean square displacement (MSD). The Einstein equation was used to calculate the ionic conductivity, σ [10, 11],

$$\sigma = \frac{e^2}{6tVkT}\left(\sum_i z_i^2 \left\langle [R_i(t) - R_i(0)]^2 \right\rangle + 2\sum_{j>i} z_i z_j \left\langle [R_i(t) - R_i(0)][R_j(t) - R_j(0)] \right\rangle\right), \qquad [4]$$

where t is the time, V, the volume of the unit cell, e, the electronic charge, k, Boltzmann's constant, T, the temperature, and z, the charge of the ions. The simulation diffusivity data are listed in Table 1. Because in the NVE ensemble the temperature could not fixed, the data listed in **Table 1** are results of extrapolations or interpolations. The experimental data in **Table 1** were collected from Refs [3] and [4]. Interpolations were performed with the experimental data to evaluate the diffusivity at the right water content.

The results of runs using the model unit cells are presented in Fig. 3. The diffusivity of hydronium evaluated using the simulation models and the experimental data are generally in good agreement with the diffusivity of hydronium evaluated previously [3, 4, 12].

Fig. 4 shows the simulation and permeability measurement results. The experimental results are very close to the results that were obtained previously by the present authors [12] and in good agreement with the results of the methanol crossover measurements by others [13]. The methanol diffusivity data that evaluated using the atomistic simulation method are generally slightly greater than the experimental permeability results. If the partitioning coefficient, H, is close to 1.0, the simulation and experiment results are in very good agreement.

Table 1. Simulation results in comparison with experimental results for 300 K from literature

Water content, λ	D_{H+}, $cm^2\ s^{-1}$	D_{H3O+}, $cm^2\ s^{-1}$	D_σ, $cm^2\ s^{-1}$ [3, 4]	D_{1H}, $cm^2\ s^{-1}$ [3, 4]
3 (Low)	$6.0 \cdot 10^{-7}$	$9.3 \cdot 10^{-7}$	$6.0 \cdot 10^{-7}$	$4.0 \cdot 10^{-7}$
13 (High)	$3.4 \cdot 10^{-6}$	$6.4 \cdot 10^{-6}$	$8.0 \cdot 10^{-6}$	$5.0 \cdot 10^{-6}$

22 (High)	$5.0 \cdot 10^{-6}$	$9.2 \cdot 10^{-6}$	$2.0 \cdot 10^{-5}$	$9.0 \cdot 10^{-6}$

Colum 1: simulation results on diffusivity of H^+; Colum 2: simulation results for H_3O^+; Colum 3: diffusion coefficient of protonated water determined using conductivity measurements [3, 4]; Colum 4: Water self-diffusivity determined using nuclear magnetic resonance (NMR) [3, 4].

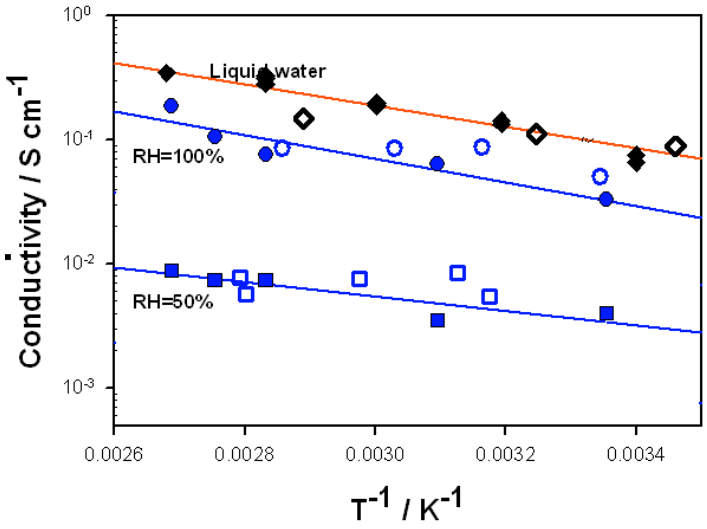

Fig. 3. Conductivity as a function of temperature and relative humidity and results of atomistic simulation. The closed symbols are experimental data points. The open symbols are simulation data points

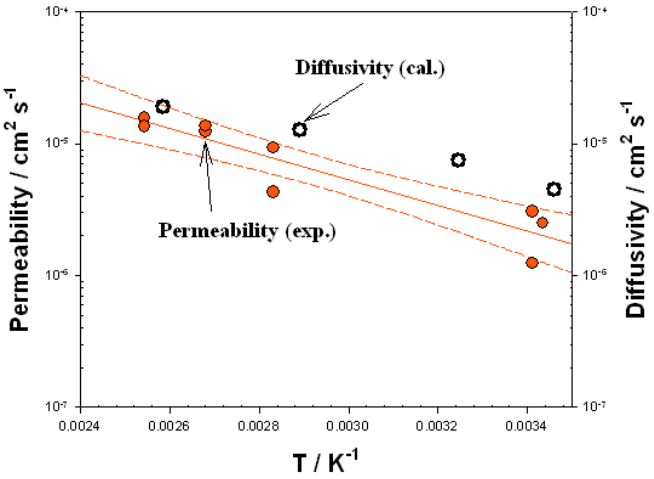

Fig. 4. Methanol permeability as a function of temperature and diffusivity data evaluated using the atomistic simulation method

Discussion and summary

Diffusivity of the protonated water in Nafion was previously evaluated using conductivity measurements [3, 4]. The data can be explained as an average of the diffusion coefficients of all existing ions in Nafion including the sulfonated groups. However, because the sulfonated groups are immobile, the contribution of their diffusion to the average diffusion coefficient is negligible. As shown in Table 1, at low water content ($\lambda = 3$), the calculated diffusivity of hydronium is 50 % greater than the experimental result reported in literature. When the water content is 13, the calculated

diffusivity of hydronium is 30 % less than the experimental result. At the highest water content (λ = 22), the calculated diffusivity of hydronium is about 50 % less than the experimental result. However, the comparison reveals a pattern that the higher the water content, the lower the calculated value in reference to the respective experimental value. It is commonly accepted that at high water contents, the structural diffusion dominates the proton transport in water and in hydrated Nafion. The comparison in Table 1 indicates that the structural diffusion may only contribute 50 % of the total diffusivity of protons at water content of 22 while negligibly at water content of 3. Because both the structural and vehicular diffusions are confined by the polymer backbones and side chains, this is not a surprising observation. Another pattern is that the diffusivity of hydrogen nuclei, D_{1H}, evaluated using a NMR method, was less than the average diffusivity of the protonated water. Although the NMR method is considered as one of the most precise methods for diffusivity measurements, it evaluates mainly the diffusivity of water. A reliable analytical relationship between the diffusivity of proton and D_{1H} is not available.

As shown in Fig. 3, the simulation conductivity data are generally consistent with the experimental results. However, there are appreciable differences between the simulation and experimental results. At some points, the differences can be 100 %. The other observation is that the simulation must underestimate the activation energies of the conduction. The primary reason for this discrepancy is that these simulation models do not take into account and interaction between the membrane itself and its environment. In reality, the water uptake at elevated temperatures may be greater than that at room temperature. In the simulations, it was assumed that both water content and density were constants for varying temperature. The second reason may be that the classical MD simulations do not involve the thermally activated chemical reactions that may contribute to the conduction of protons, structural diffusion, and dissociation of protons from the sulfonated groups.

The simulation models correctly predict the diffusivities of hydronium and methanol in a wide range of temperature (Fig. 4). Methanol is a neutral species and weakly interacts with Nafion backbone. It is not surprising that the present MD models that do not consider chemical interaction between the molecules can still correctly evaluate the diffusivity of methanol.

The summary is as follows. The simulations can predict the conductivity of Nafion, diffusivity of hydronium, and methanol diffusivity in Nafion in a temperature range between 20 and 120 °C with the maximum error of 50 % at room temperature or 100 % at higher temperatures. The computational conductivity results gradually deviate from the experimental values with increasing temperature and water content. The contribution of structural diffusion to the proton mobility is only 50 % in Nafion. Methods that can describe the structural diffusion are needed to predict the transport properties of Nafion at high water content (λ>22).

DIFFUSION AT THE INTERFACIAL AREA BETWEEN A NAFION CLUSTER AND CARBON SUPPORT

Diffusion of reactants and products in the catalyst layers in PEFCs is a very important academic and practical issue. Appropriate amount of moisture or water should be supplied to the vicinity of the anodic catalysts on carbon support in conjunction with Nafion clusters to compensate the hydration loss due to electroosmotic drag of water. However, the water supply should be tuned to a level that does not flood the interfacial area and impede the diffusion of hydrogen to the Pt catalysts. In the cathodic catalyst layer, water as a product of the cathodic reaction should be removed and rejected. Continuum models have had some successes in theoretical analyses of the GDLs. These models generally assume that the materials properties of Nafion clusters in the catalyst layer are similar to that of the macroscopic Nafion membrane. However, this assumption should be verified.

An interface model created using Discover™ is shown in Fig. 5. The Nafion cluster is sandwiched between two carbon slabs with a face index of (1 1 1) and distance of 10 nanometers. The Nafion cluster was created earlier with a water content of 4 and contained hydronium, water, methanol, hydrogen, and oxygen. This free Nafion cluster was used as the baseline for this simulation work. Then the Nafion cluster was transferred between the carbon slabs and reconciled using the energy minimization method. The surface atoms of the carbon slabs can be charged to mimic the situations when the catalyst layers are charged during operation. In our studies the charge density varies from 0.00005 to 0.05 e per surface atom.

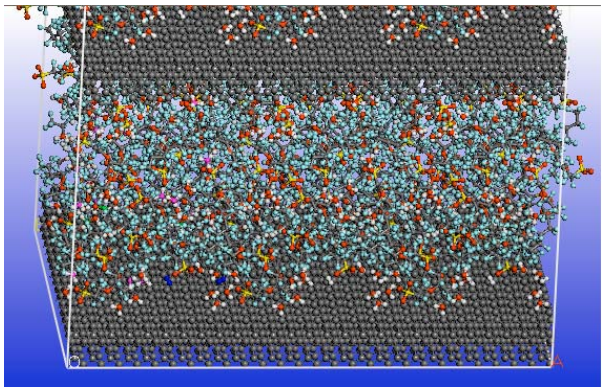

Fig. 5. A MD model of a Nafion cluster sandwiched between two carbon slab with a face index of (1 1 1)

Table 2. Computational results of diffusivities of species in the Nafion cluster in the model shown in Fig. 5.

Charge per surface C atom, e	D_{H_2}, cm^2/s	D_{O_2}, Cm^2/s	$D_{H_3O^+}$, cm^2/s	D_{H_2O}, cm^2/s	D_{CH_3OH}, cm^2/s
-0.0005	$2.92 \cdot 10^{-4}$	$3.46 \cdot 10^{-6}$	$5.98 \cdot 10^{-6}$	$1.68 \cdot 10^{-5}$	$1.43 \cdot 10^{-5}$
-0.005	$2.47 \cdot 10^{-4}$	$7.04 \cdot 10^{-6}$	$8.95 \cdot 10^{-6}$	$2.57 \cdot 10^{-5}$	$2.10 \cdot 10^{-5}$
0.0	$2.47 \cdot 10^{-4}$	$8.22 \cdot 10^{-6}$	$1.26 \cdot 10^{-5}$	$2.89 \cdot 10^{-5}$	$2.04 \cdot 10^{-5}$
0.00005	$5.96 \cdot 10^{-4}$	$2.11 \cdot 10^{-5}$	$1.16 \cdot 10^{-5}$	$3.04 \cdot 10^{-5}$	$1.49 \cdot 10^{-5}$
0.01	$2.10 \cdot 10^{-4}$	$1.67 \cdot 10^{-5}$	$4.73 \cdot 10^{-6}$	$9.50 \cdot 10^{-6}$	$1.16 \cdot 10^{-5}$
0.05	$2.53 \cdot 10^{-4}$	$1.70 \cdot 10^{-6}$	$6.12 \cdot 10^{-6}$	$1.04 \cdot 10^{-5}$	$1.75 \cdot 10^{-5}$
Free Nafion cluster	$6.83 \cdot 10^{-5}$	$1.09 \cdot 10^{-5}$	$2.60 \cdot 10^{-6}$	$6.38 \cdot 10^{-6}$	$5.31 \cdot 10^{-6}$

Discussion and summary

The last line of Table 2 gives that data obtained in a case when there is no presence of carbon. The diffusivity of hydrogen in Nafion 117 at 300 K, 1 atmosphere, and a relative humidity of ~60 % is $6.83 \cdot 10^{-5}$ cm^2/s. According to the hydrogen crossover data in Nafion membrane published by Cheng et al [14] and Henry's constants published by Mann et al [15], the diffusivity of hydrogen in Nafion should be $9.0 \cdot 10^{-5}$ cm^2/s under similar conditions. Thus, the present simulation result for free Nafion cluster is in a good agreement with the experimental results. According Cheng et al [14], the diffusivity of hydrogen in catalyst layer should be in the order of 10^{-4} cm^2/s. The present results for diffusion of hydrogen are generally consistent with the experimental observations. For diffusion of oxygen in Nafion, the datum reported by Secanell et al [16] is $8.45 \cdot 10^{-6}$ cm^2/s which is also close to the value of $1.09 \cdot 10^{-5}$ cm^2/s evaluated using the MD simulation method.

The data in Table 2 indicate that the diffusivity of hydrogen in Nafion cluster between the carbon slabs are nearly 3-8 times greater than that in a free Nafion cluster. Increase in diffusivity in Nafion cluster between carbon slabs is a generic phenomenon for other species including oxygen, hydronium, water and methanol. This may be explained by the strong interaction between the Nafion cluster and the carbon slabs. An evidence of collective vibrations of the carbon slabs is illustrated in Fig. 6 where the mean square displacement (MSD) of the carbon slab fluctuates with time. The vibrations of the entire piece of carbon slab may cause a "tossing" effect that enables a higher mobility of the atoms in the Nafion cluster. It is interesting that the maximum diffusivity appears when the magnitude of charge density is low or zero. The charges on the carbon slabs attract some of charged species (hydronium and sulfonated groups) and polar species (water and methanol) and may impede the movement of the other species.

In summary, diffusivities of hydrogen, methanol, and hydronium in the nanoscale interfacial area between a Nafion cluster and carbon support can be much greater than those in a bulk Nafion cluster or membrane. This may have a significant impact on the continuum models of the transport processes in the catalyst layer and in GDLs.

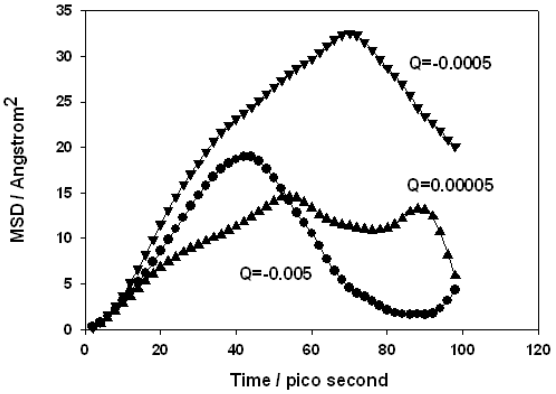

Fig. 6. MSDs of the carbon slabs in the model shown in Fig. 5 fluctuate with time. The numbers are the charges on a surface atom

DISINTEGRATION AND RE-PRECIPITATION OF PLATINUM CATALYSTS DURING CHARGING AND DISCHARGING PROCESSES

Background

The activity loss of catalysts in of PEFCs has been recently recognized as one of the most important issues to be addressed before the commercialization of the PEFC based power sources [17, 18]. Recent studies invoked the dissolution of Pt nano-crystallites and re-crystallization or redeposition of Pt ions to explain the experimental observations. Ferreira et al. [17, 18] proposed that coarsening of Pt particles was via two different processes: 1) Ostwald ripening on carbon support via transport of soluble Pt species at the nanometer scale, which was responsible for platinum particle coarsening from 2 to 6 nm on carbon, and 2) migration of soluble platinum species in the ionomer phase at the micrometer scale, chemical reduction of these species by crossover H_2 molecules, and precipitation of platinum particles in the cathode ionomer phase. Results of experimental studies by Taniguchi et al. [19] and Akita et al. [20] support the theory qualitatively. Another noticeable observation was that cycling the potential of the electrodes, in particular that of the cathode, significantly accelerated the loss of electrochemical activity (ECA). However, Pt is known as a very stable metal. The prediction using Pourbaix diagram gives an equilibrium soluble Pt concentration one order of magnitude and two orders of magnitude lower than the data from equilibrium solubility measurements at respectively 0.9 and 0.85 V versus reversible hydrogen electrode (RHE) [17]. The measured potential dependence of Pt concentration does not follow the Nernstian behavior. In addition, the rate of loss under potential cycling predicted by the dissolution/re-deposition mechanism is 1-4 orders of magnitude lower than the observed value [17, 21, 22]. A recent continuum model [23] has considered (1) dissolution of Pt and subsequent electrochemical redeposition on Pt nanoparticles in cathode; (2) diffusion of Pt ions in the membrane electrode assembly (MEA); and (3) Pt ion chemical reduction in membrane by hydrogen permeating through the membrane from the negative electrode. However, there are large discrepancies between the theoretical predictions and experimental observations. This leads us to re-examine the mechanism of loss of ECA using a MD method.

Molecular dynamic (MD) simulation model

A typical MD model created using Discover^{TM} with a periodic boundary condition is shown in Fig. 7. Because of the use of the periodic boundary condition, the upper Pt lattice in fact joins with the lower Pt lattice at the top face of the upper Pt lattice and bottom face of the lower Pt lattice. Thus, the unit cell consists of two parts: the platinum lattice and a Nafion electrolyte cluster in the middle. The top and bottom face of the Pt lattice has a Miller index of (11-2). The size of the Pt lattice was 2.6 nm long x 1.4 nm wide x 0.6 nm thick, similar to the size of the average Pt particles in pristine PEFC catalyst layers. This model is meant to mimic a Pt nano-crystallite outcropping into the Nafion electrolyte. The creation of the Nafion electrolyte cluster was described in detail in first two sections. The water ratio was set at 4 which was corresponding to the equilibrium hydration level at a relative humidity of ~60 %. The unit cell was optimized by minimizing the total potential energy. After energy minimization, the Pt lattice has already shown slight distortion due to the interaction between the Pt lattice and Nafion cluster.

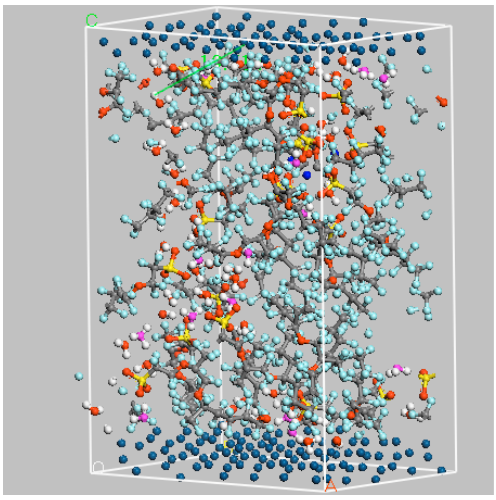

Fig. 7. Unit cell of a Pt-Nafion electrolyte interface model. The surface of the Pt lattice has a Miller index of (11-2). The water ratio of the Nafion cluster is 4 corresponding to the equilibrium value at 60 % relative humidity at room temperature

Prior to a MD simulation run, the Pt lattice in the equilibrium unit cell was charged. The charging process is meant to mimic a potential ramp in a potential cycle of square waveform. The amount of charge or charge density was estimated as follows. According to published data of electrochemical impedance spectroscopy study on PEFC electrode layers, the double layer capacitance is about 20 $mF \cdot cm^{-2}$ [23]. The ECA of the catalysts layer is about 70 $m^2 \cdot g^{-1}$ [17, 18]. The catalyst loading was 0.4 $mg \cdot cm^{-2}$. Thus, the ratio of ECA to the area of catalyst layer in the MEA is 280 $cm^2_{Pt} \cdot cm^{-2}_{MEA}$. The charge density is evaluated using:

$$Q = CV \tag{5}$$

where Q is charge density, C is area specific double layer capacitance, and V is the interfacial potential difference. In order to estimate the charge density, it is assumed that the interfacial potential difference is 0.5 V. At this potential difference Q is about 0.01 $C \cdot cm^{-2}_{MEA}$ or $3.57 \cdot 10^{-5}$ $C \cdot cm^{-2}_{Pt}$ or 2.23×10^{-2} e $angstrom^{-2}_{Pt}$. The base area of the unit cell is 364 $angstrom^2$. Thus, the charge on the unit cell is +8.12 e. Considering the Pt lattice has two interfaces with the Nafion clusters, the total charge should be about +16 e. However, this method may underestimate the charge density for smaller Pt crystallites while it may overestimate the charge density for larger Pt crystallites because the charges tend to concentrate at smaller Pt crystallites if the surfaces of the small and large Pt crystallites are at the same electrical potential on the carbon support. Thus, charge density may be expected to be many times greater than +16 e per unit cell area for small Pt crystallites when the electrode is charged.

Simulation results and discussions

The temperature was initially set at 350 K (76.9 ºC) under NVE ensemble with constant particle number, constant volume (1 bar), and constant energy. However, the final temperature was usually higher than the initial temperature. The charge of the Pt lattice is altered from zero to a finite value, mimicking a potential ramp. The initial velocity was randomly determined according to Boltzmann statistics. The time step was set at 1.0 fs and duration at 200 ps. Fig. 8 a shows the unit cell charged with +32 e at 25 ps. The crystalline structure is almost completely disintegrated with some small Pt clusters and individual Pt ions separating from the main body of the Pt lattice. Fig. 8 b shows the unit cell with +64 e at only 15 ps. The Pt lattice is completely separated into small Pt clusters and ions. Similar results were also obtained when the Pt lattice was negatively charged.

It is not difficult to envision that the interaction between the Nafion electrolyte and Pt nano-crystallites can cause distortion of the periodic lattice of Pt. If the Pt is positively charged, the electrical field tends to push the protons or hydroniums away from the Pt lattice while drag the sulfonated groups closer. The simulation results clearly reveal that sulfonated groups that have certain stiffness penetrate the lattice (Fig. 8). If the Pt lattice is negatively charged, the protons or hydroniums will penetrate the Pt lattice. If the Pt lattice is larger, the Pt lattice is distorted to a lesser extent and the charged species in Nafion are less likely to penetrate the Pt lattice. As shown in Fig. 9, the Pt lattice that is two times thicker than those in Fig. 8 is almost intact at a charge of +32 e after 175 ps. Thus, larger Pt particles are less likely to be disintegrated by the interaction between the charged Pt lattice and polarized Nafion cluster. This process of distortion, disintegration, and complete separation may

be very difficult to be viewed with available *ex situ* analytical methods (SEM, TEM, XRD, etc.). However, it can be visualized using a virtue test conducted using a MD simulation.

a) b)

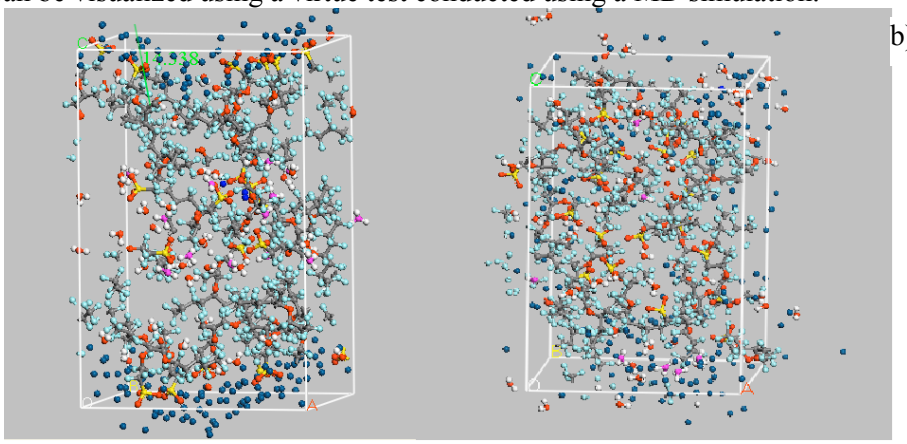

Fig. 8. a) – Configuration of the unit cell with a charge of +32 e on the Pt lattice at 25 ps.
b) – Configuration of the unit cell with a charge of +64 e on the Pt lattice at 15 ps

As can be seen in Fig. 8, the Pt ions diffuse in the Nafion cluster. Previous studies [17-20] indicate the Pt ions can be reduced by crossover hydrogen that transport from anode to cathode and the Pt atoms may re-precipitate on carbon support or inside the Nafion electrolyte. If the newly formed Pt crystallites on the carbon support are recharged, they will undergo the same processes of disintegration unless the crystallites become large enough by chance. The newly formed Pt crystallites in Nafion electrolyte are excluded from the electrochemical processes and hence become stable or keep growing at the expense of the smaller Pt nano-crystallites on the carbon support [17-20]. Both of these processes result in loss of ECA.

This re-precipitation process can also be simulated using MD method. The configuration shown in Fig. 10a was inherited from a configuration with a distorted Pt lattice and some separate Pt atoms in the Nafion cluster. The charge on the Pt was removed and a MD run was initiated. After 0.4 ns, Pt atoms that used to be at the left bottom corner join the largest Pt lattice. The Pt lattice that used to be non-periodic when it was charged regained its periodicity. However, other separate Pt atoms aggregated at the middle of the Nafion cluster. The outcome of a charging/discharging cycle is that most of Pt atoms remain in the bulk of Pt slab but some remain in the Nafion cluster and lose electrical connection with the Pt lattice. It is worthy noticing that the precipitation process is much slower than the disintegration process.

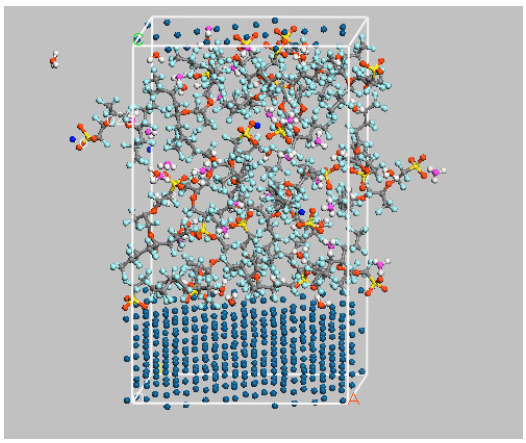

Fig. 9. Configuration of a unit cell with a thicker (1.2 nm) Pt lattice at 175 ps. The Pt lattice carries a positive charge of 32 e

a) 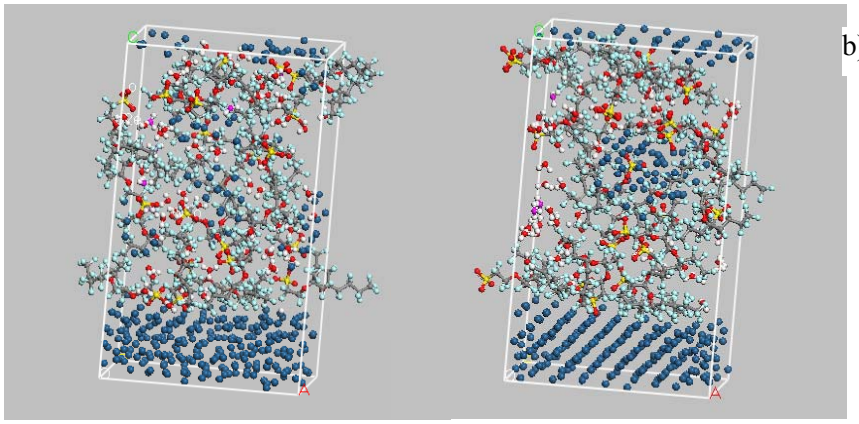 b)

Fig. 10. a) Left: An atomistic model with neutral Pt atoms scattering randomly in a Nafion cluster as a consequence of disintegration. b) Right: After 400 picoseconds, the Pt atoms spontaneously aggregate to form 2 clusters and regain periodicity

Summary

The MD simulations reveal that charged Pt nano-crystallites in the catalyst layers of a PEFC can undergo instantaneous disintegration under mainly electrostatic interaction between charged Pt nano-crystallites and polarized polymer electrolyte. Larger Pt crystallites are more likely to survive disintegration than smaller Pt crystallites. The MD simulation can also simulate the re-precipitation of the discharged Pt atoms. The results indicate that the re-precipitation process is a much longer process than the disintegration process.

References

1. Adam Z. Weber and John Newman. Transport in Polymer-Electrolyte Membranes I. Physical Model // *J. of The Electrochemical Society*. 2003. Vol. 150 (7). Pp. A1008-A1015.
2. Adam Z. Weber and John Newman. Transport in Polymer-Electrolyte Membranes II. Mathematical Model // *J. of The Electrochemical Society*, 2004. Vol.151(2). Pp. A311-A325.
3. Klaus-Dieter Kreuer, Stephen J. Paddison, Eckhard Spohr, and Michael Schuster. Transport in Proton Conductors for Fuel-Cell Applications: Simulations, Elementary Reactions, and Phenomenology // *Chem. Rev*., 2004, Vol.104, pp. 4637-4678.
4. Kreuer K.D.. Fast proton conductivity: A phenomenon between the solid and the liquid state? // *Solid State Ionics*, 1997, Vol.94, pp. 55-62.
5. Seeliger, D.C. Hartnig, Spohr E.. Aqueous pore structure and proton dynamics in solvated Nafion membranes // *Electrochimica Acta*, 2005, Vol.50, pp. 4234-4240.
6. Walbran S. and Kornysheva A. A.. Proton transport in polarizable water // *J. Chem. Phys*., 2001, Vol. 114(22), Pp.0039–10048.
7. Tuckerman Mark, Laasonen Kari, Sprik Michiel, and Parrinello Michele. Ab initio molecular dynamics simulation of the solvation and transport of hydronium and hydroxyl ions in water // *J. Chem. Phy.*, 1995, Vol.103, pp. 150-161.
8. Joseph A. Morrone, Mark E. Tuckermana, Ab initio molecular dynamics study of proton mobility in liquid methanol // *J. Chem. Phys*., 2002, Vol. 117(9), 4403-4413.
9. Ennari Jaana, Elomaa Matti, and Sundholm Franciska. Modelling a polyelectrolyte system in water to estimate the ion-conductivity // *Polymer*, 1999, Vol.40, pp. 5035–5041.
10. Lapid H., Agmon N., Petersen M., and Voth S.. A bond-order analysis of the mechanism for hydrated proton mobility in liquid water // *J. Chem. Phys.*, 2005, Vol.122, pp. 014506-1-11.
11. Allen Michael P., Introduction to Molecular Dynamics Simulation published in Computational Soft Matter: From Synthetic Polymers to Proteins, Lecture Notes, Norbert Attig, Kurt Binder, Helmut Grubm¨ uller, Kurt Kremer (Eds.), John von Neumann Institute for Computing, J ¨ ulich, NIC Series, ISBN 3-00-012641-4, 2004, Vol.23, pp. 1-28.
12. Xiangyang Zhou, Jamie Weston, Elena Chalkova, Michael A. Hofmann, Catherine M. Ambler, Harry R. Allcock, and Serguei N. Lvov. High Temperature Transport Properties of

Polyphosphazene Membranes for Direct Methanol Fuel Cells // *Electrochimica Acta*, 2003, Vol.48 , pp. 2173-2180.
13. Ren X., Zawodzinski T.A., Uribe F., Dai H., Gottesfeld S., Methanol crossover in direct methanol fuel cells, in: S. Gottesfeld, G. Halpert, A. Landgrebe Eds., Proton Conducting Membrane Fuel Cells I, The Electrochemical Society Proceedings Series, Pennington, NJ., 1995, Vol. 95, pp. 284–298.
14. Xuan Cheng, Jianlu Zhang, Yanghua Tang, Chaojie Song, Jun Shen, Datong Song, Jiujun Zhang. Hydrogen crossover in high-temperature PEM fuel cells // Journal of Power Sources, 2007, Vol.167, pp. 25–31.
15. Mann R.F., Amphlett J.C., Peppley B.A., Thurgood C.P.. Henry's Law and the solubilities of reactant gases in the modelling of PEM fuel cells // *J. of Power Sources*, 2006, Vol.161, pp. 768–774.
16. Secanell M., Karan K., Suleman A., Djilali N.. Multi-variable optimization of PEMFC cathodes using an agglomerate model // *Electrochimica Acta*, 2007, Vol.52, pp. 6318–6337.
17. Ferreira P. J., la O' G. J., Shao-Horn Y., Morgan D., Makharia R., Koch S., and Gasteiger H. A. Instability of Pt/C Electrocatalysts in Proton Exchange Membrane Fuel Cells: A Mechanistic Investigation // *J. of The Electrochemical Society*, 2005, Vol.152(11), pp. A2256-A2271.
18. Shao-Horn Y., Ferreira P.J., la O G.J., Morgan D., Gasteiger H., Makharia R.. Coarsening of Pt Nanoparticles in Proton Exchange Membrane Fuel Cells Upon Potential Cycling // ECS *Transactions*, 2006, Vol.1(8), pp. 185-195.
19. Taniguchi A., Akita T., Yasuda K., Miyazaki Y., Analysis of electrocatalyst degradation in PEMFC caused by cell reversal during fuel starvation // *J. Power Sources*, 2004, Vol.130**,** pp. 42-49.
20. Tomoki Akita, Akira Taniguchi, Junko Maekawa, Zyun Siroma, Koji Tanaka, Masanori Kohyama, Kazuaki Yasuda. Analytical TEM study of Pt particle deposition in the proton-exchange membrane of a membrane-electrode-assembly // *Journal of Power Sources*, 2006, Vol.159, pp. 461–467.
21. Robert M. Darling and Jeremy P. Meyers. Kinetic Model of Platinum Dissolution in PEMFCs // *J. of The Electrochemical Society*, 2003. Vol.150 (11). Pp. A1523-A1527.
22. Robert M. Darling and Jeremy P. Meyers. Mathematical Model of Platinum Movement in PEM Fuel Cells // *J. of The Electrochemical Society*, 2005. Vol.152(1), A242-247.
23. Wu Bi, Thomas F. Fuller. Modeling of PEM fuel cell Pt/C catalyst degradation // *J. of Power Sources.* 2008. Vol.178. Pp. 188–196.